Virology 291, 110–125 (2001)
doi:10.1006/viro.2001.1194, available online at http://www.idealibrary.com on IDEAL®

Functional Analysis of Proteins Involved in Movement of the Monopartite Begomovirus, *Tomato Yellow Leaf Curl Virus*

Maria R. Rojas,*,† Hao Jiang,* Raquel Salati,* Beatriz Xoconostle-Cázares,† M. R. Sudarshana,* William J. Lucas,† and Robert L. Gilbertson*,[1]

*Department of Plant Pathology, University of California, Davis, California 95616; and †Section of Plant Biology, Division of Biological Sciences, University of California, Davis, California 95616

Received July 5, 2001; returned to author for revision August 8, 2001; accepted September 12, 2001; published online

The functional properties of proteins [capsid protein (CP), V1, and C4] potentially involved with movement of the monopartite begomovirus, *Tomato yellow leaf curl virus* (TYLCV), were investigated using microinjection of *Escherichia coli* expressed proteins and transient expression of GFP fusion proteins. The TYLCV CP localized to the nucleus and nucleolus and acted as a nuclear shuttle, facilitating import and export of DNA. Thus, the CP serves as the functional homolog of the bipartite begomovirus BV1. The TYLCV V1 localized around the nucleus and at the cell periphery and colocalized with the endoplasmic reticulum, whereas C4 was localized to the cell periphery. Together, these patterns of localization were similar to that of the bipartite begomovirus BC1, known to mediate cell-to-cell movement. However, in contrast to BC1, V1 and C4, alone or in combination, had a limited capacity to move and mediate macromolecular trafficking through mesophyll or epidermal plasmodesmata. Immunolocalization and *in situ* PCR experiments, conducted with tomato plants at three stages of development, established that TYLCV infection was limited to phloem cells of shoot apical, leaf, stem, and floral tissues. Thus, the V1 and/or C4 may be analogs of the bipartite begomovirus BC1 that have evolved to mediate TYLCV movement within phloem tissue.

Key Words: begomovirus; capsid protein; geminivirus; green fluorescent protein; immunolocalization; microinjection; movement protein; plant virus movement; phloem-limited virus; plasmodesmata; TYLCV.

INTRODUCTION

To establish a systemic infection, plant viruses must interact with the host plant for replication, gene expression, and cell-to-cell and long-distance movement. During this process, the virus must overcome the barrier to cell-to-cell movement presented by the cell wall. To this end, plant viruses encode movement proteins (MPs) that can interact with plasmodesmata (PD), the plasma membrane-lined channels that interconnect plant cells, to facilitate the cell-to-cell transport of the infectious form of the virus (Lucas and Gilbertson, 1994). At present, two distinct mechanisms have been described for viral cell-to-cell movement through PD (Lucas and Gilbertson, 1994; Carrington *et al.,* 1996; Lazarowitz and Beachy, 1999). One mechanism involves the MP interacting with the viral nucleic acids to form an MP–nucleoprotein complex that is capable of passing to the next cell via PD (Ghoshroy *et al.,* 1997; McLean *et al.,* 1997). The second mechanism involves virus particles that appear to move in conjunction with the formation of tubular structures that extend into the cytoplasm of adjacent uninfected cells (e.g., Kasteel *et al.,* 1996). Long-distance movement occurs as the virus moves out of an inoculated tissue to other regions of the plant, and this is usually via the phloem. The CP is necessary for long-distance movement of the majority of viruses, but it is not known whether this reflects a role for virions in this process or some other role, such as the formation of a nonvirion movement complex (Gilbertson and Lucas, 1996; Nelson and van Bel, 1998).

Geminiviruses (family Geminiviridae) are one of the few groups of plant-infecting viruses that possess a single-stranded (ss)-DNA genome. Thus, geminiviruses have evolved mechanisms to mediate the cell-to-cell and long-distance transport of DNA in plants. For the bipartite members of the genus *Begomovirus*, which have genomes composed of two circular 2.5- to 2.8-kb ss-DNA molecules (designated DNA-A and DNA-B), cell-to-cell movement requires two proteins encoded by the DNA-B component, BV1 and BC1 (Brough *et al.,* 1988; Etessami *et al.,* 1988; Jeffrey *et al.,* 1996; Sudarshana *et al.,* 1998). Unlike many viruses, the CP of bipartite begomoviruses is not required for cell-to-cell or long-distance movement (Azzam *et al.,* 1994; Gardiner *et al.,* 1988; Ingham *et al.,* 1995; Padidam *et al.,* 1995; Sudarshana *et al.,* 1998). *Bean dwarf mosaic virus* (BDMV) is a bipartite begomovirus that is not phloem-limited and is readily sap-transmissible (Wang *et al.,* 1996; Sudarshana *et al.,* 1998). Microin-

[1] To whom correspondence and reprint requests should be addressed. Fax: (530) 752-5674. E-mail: rlgilbertson@ucdavis.edu.

0042-6822/01 $35.00

jection studies with *Escherichia coli* expressed proteins have established that BV1 accumulates in the nucleus and mediates nuclear import and export of DNA, whereas BC1 moves through mesophyll PD and mediates cell-to-cell movement of DNA (Noueiry *et al.,* 1994; Rojas, 1999). *In vitro* DNA binding studies demonstrated that both BDMV BV1 and BC1 bind ss- and double-stranded (ds)-DNA and that binding occurs in a size- and form-specific manner (Rojas *et al.,* 1998). These findings have led to a model for BDMV cell-to-cell movement in which BV1 exports nascent ss- and/or ds-viral DNA from the nucleus, BC1 mediates cell-to-cell movement of the viral DNA via PD, and the concerted action of BV1 and BC1 is involved in the maintenance of genome size. A somewhat different model for *Squash leaf curl virus* (SLCV), a phloem-limited bipartite begomovirus, has been proposed in which BV1 shuttles viral ss-DNA from the nucleus to the cytoplasm, and BC1 traps BV1–ss-DNA complexes and mediates their cell-to-cell spread via ER-derived tubules (Lazarowitz and Beachy, 1999). Thus, the cell-to-cell movement of bipartite begomoviruses does not require the CP (and therefore virions), but requires two proteins (BV1 and BC1) that mediate nuclear and cell-to-cell transport, respectively. The different tissue tropisms (i.e., phloem-limited vs non-phloem-limited) exhibited by bipartite begomoviruses may reflect specific mechanisms of movement or differences in efficiency of movement (Morra and Petty, 2000).

Tomato yellow leaf curl virus (TYLCV) is one of the few begomoviruses that possesses a monopartite genome (Navot *et al.,* 1991). The TYLCV genome consists of a single ~2.8-kb circular ss-DNA that contains six open reading frames (ORFs) encoding putative proteins ~ 10 kDa or greater, located on the viral or complementary sense strands of the ds-replicative form (RF) DNA. ORFs V1 and V2 are in the virion sense, and the V2 ORF encodes the capsid protein (CP). The arrangement of the complementary sense TYLCV ORFs is similar to that of the DNA-A component of the bipartite begomoviruses, with ORFs C1, C2, and C3 partially overlapping, and a small ORF, C4, located within the C1 ORF, but in a different reading frame (Navot *et al.,* 1991). TYLCV is generally considered to be phloem-limited (Cohen and Antignus, 1994), but a recent immunolocalization study suggested that TYLCV may not be phloem-limited in all tissue types (Michelson *et al.,* 1997).

The lack of a DNA-B component may reflect fundamental differences in the tissue tropism and/or mechanism(s) of movement of monopartite vs bipartite begomoviruses. Genetic analyses of *Tomato yellow leaf curl Sardinia virus* (TYLCSV), a species closely related to TYLCV and with a similar genome organization, have suggested that as many as four ORFs may be involved in viral movement: V1, V2 (*CP* gene), C2, and C4 (Jupin *et al.,* 1994; Wartig *et al.,* 1997). Disruption of the TYLCSV *CP* gene abolished symptom development and accumulation of viral DNA in *Nicotiana benthamiana* and tomato plants (Wartig *et al.,* 1997). Furthermore, results obtained with CP mutants of a TYLCSV isolate from Sicily suggested that virions may be required for systemic infection (Noris *et al.,* 1998). TYLCSV V1 mutants induced symptomless infections and had reduced levels of DNA in *N. benthamiana* plants, but were essentially not infectious in tomato (Wartig *et al.,* 1997). Similarly, TYLCSV C2 and C4 mutants also were not infectious in tomato plants, but induced attenuated symptoms in *N. benthamiana* plants (Jupin *et al.,* 1994; Wartig *et al.,* 1997). Genetic analyses of another monopartite tomato-infecting begomovirus, *Tomato leaf curl virus* (TLCV), established that the CP is required for systemic infection, whereas V1 and C4 mutants induced symptomless or attenuated systemic infections, respectively, in tomato plants (Rigden *et al.,* 1993, 1994). Collectively, these results indicate that the CP is essential for systemic infection by monopartite begomoviruses. In addition, V1, C2, and/or C4 also may be involved in movement (directly or indirectly). The TYLCV C2 has ~65% amino acid sequence identity with the AC2 (transactivator) proteins of bipartite begomoviruses, whereas none of the TYLCV genes/proteins share obvious homology to BV1 or BC1 (e.g., <42% nucleotide and <46% amino acid sequence similarities with BDMV BV1 and BC1) or identifiable shared amino acid motifs (Salati, 2001).

In this study, we present a functional analysis of the proteins potentially involved in movement of an isolate of TYLCV from the Dominican Republic (TYLCV-DO, hereafter referred to as TYLCV). Our results suggest a specific role for the CP, V1, and C4 in TYLCV movement and, on the basis of these results, potential functional homologues (BV1 or BC1) in the bipartite begomoviruses were identified. Moreover, as TYLCV was phloem-limited in tomato in various tissue types at different plant developmental stages, a model is presented in which the TYLCV utilizes a movement system adapted to the vasculature.

RESULTS

TYLCV V1 and C4 proteins exhibit limited cell-to-cell movement properties in mesophyll and epidermal cells

The TYLCV C4, V1, and CP proteins were expressed in and purified from *E. coli. E. coli* cells transformed with recombinant plasmids having the TYLCV C4 (pC4), V1 (pV1), or CP (pCP) expressed fusion proteins of the expected molecular weights: 15 kDa (C4), 17 kDa (V1), and 34 kDa (CP), respectively (Fig. 1A). No protein bands of equivalent intensities were observed in extracts prepared from *E. coli* cells transformed with pRSETA alone (Fig. 1A). For microinjection studies, proteins were covalently labeled with fluorescein isothiocyanate (FITC)-Oregon Green (OG). The functional properties of mesophyll PD in mature tomato and *N. benthamiana* leaves

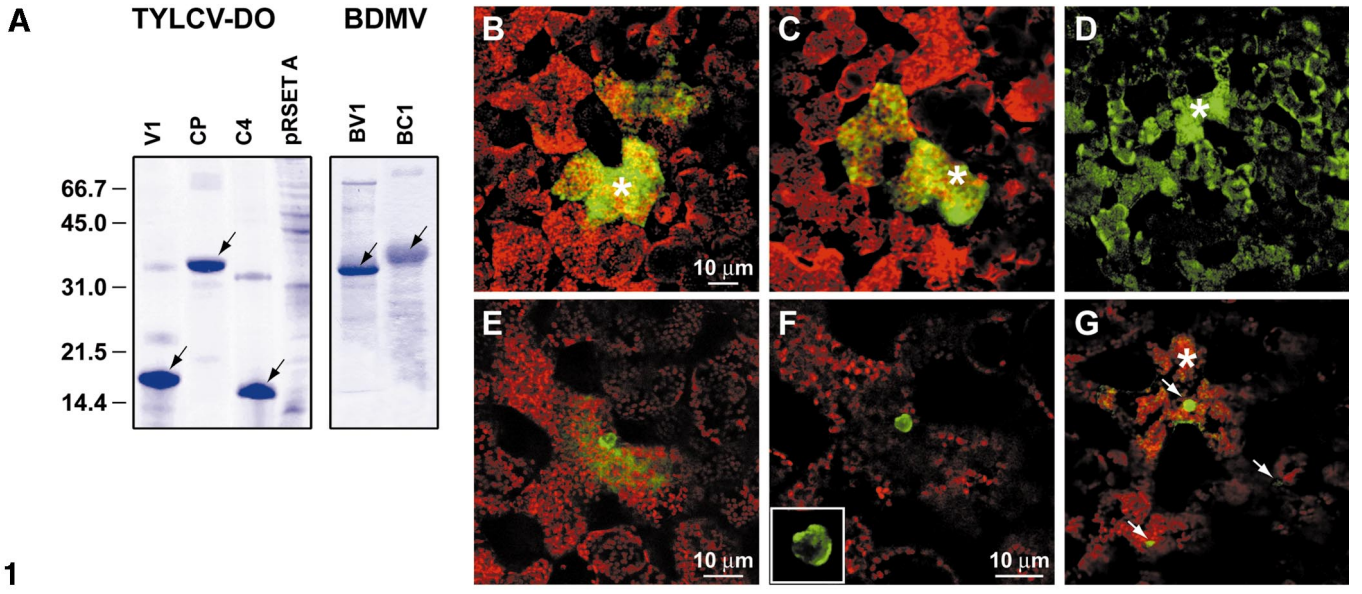
A
TYLCV-DO
BDMV
V1
CP
C4
pRSET A
BV1
BC1
66.7
45.0
31.0
21.5
14.4
B
C
D
E
F
G
10 μm
10 μm
10 μm

1

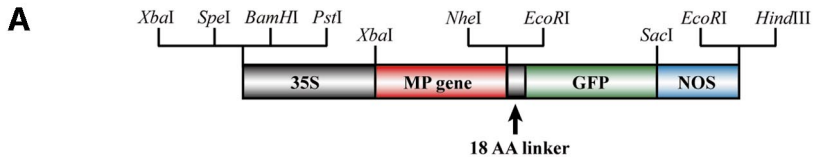
A
XbaI
SpeI
BamHI
PstI
XbaI
NheI
EcoRI
SacI
EcoRI
HindIII
35S
MP gene
GFP
NOS
18 AA linker

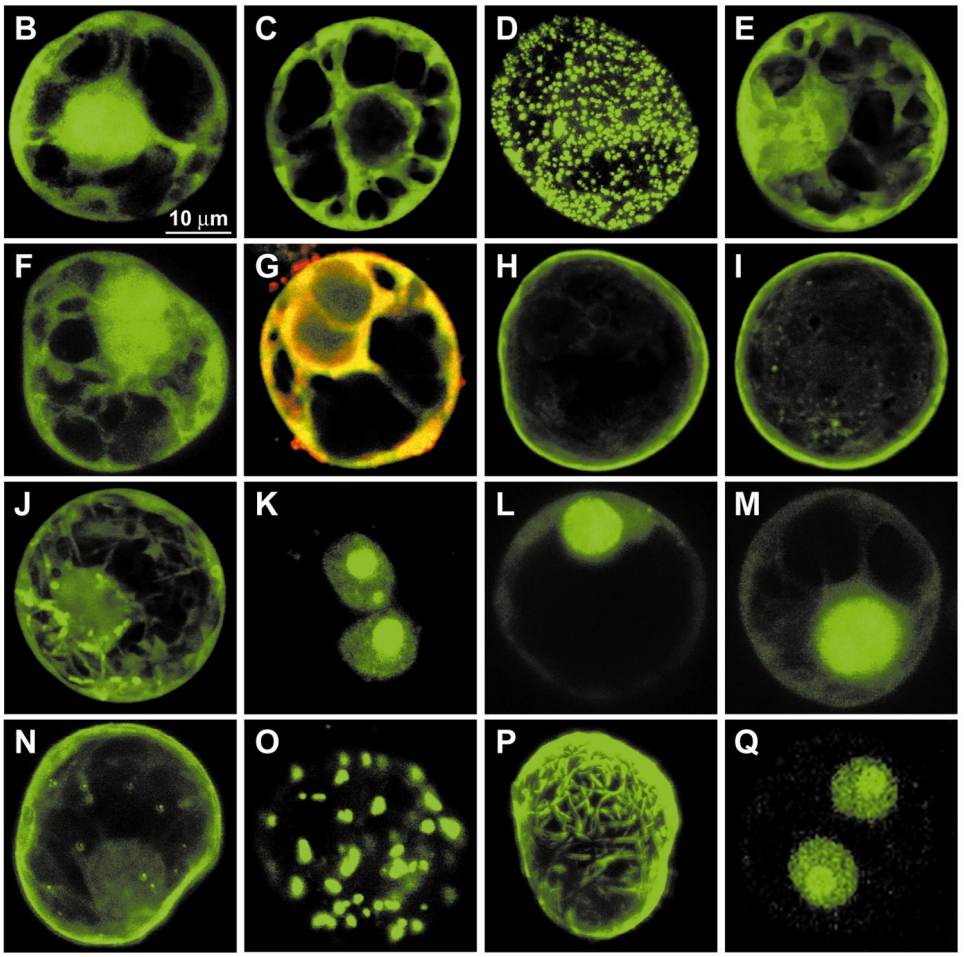
B
C
D
E
10 μm
F
G
H
I
J
K
L
M
N
O
P
Q

2

were first evaluated in control experiments as previously described (Rojas *et al.,* 1997). Here, Lucifer yellow CH (LYCH, 522 Da) was observed to move extensively, cell to cell, whereas the 4- and 10-kDa F-dextrans remained confined to the injected cells (Table 1).

When introduced into equivalent *N. benthamiana* or tomato mesophyll cells, OG-labeled C4 (OG-C4) or OG-labeled V1 (OG-V1) generally remained restricted to the injected cell. In some cases, OG-C4 (20%) or OG-V1 (25–28%) exhibited limited movement based upon detection of fluorescence in cells adjacent to the microinjected cell (Figs. 1B and 1C, Table 1). This form of interaction between the viral protein and PD, in which the protein traffics only into adjacent cells, was defined as movement that is limited to adjacent cells (LTAC). To confirm that LTAC movement was an inherent property of the C4 and V1 proteins, as opposed to a problem with PD in these tissues, control experiments were next performed with the BDMV BC1 MP, which is capable of extensive cell-to-cell movement in mesophyll tissue (Noueiry *et al.,* 1994). In such control experiments, the OG-BC1 protein underwent extensive cell-to-cell movement (Fig. 1D, Table 1), confirming the functional status of the mesophyll PD.

Recently, it was suggested that the capacity of PD to mediate in the trafficking of macromolecules may well depend upon the physiological status of the leaf (Oparka *et al.,* 1999). For example, in sink leaves, proteins of up to 50 kDa were reported to freely move through PD. To test whether the TYLCV C4 or V1 proteins would exhibit more extensive cell-to-cell movement properties in sink tissues, microinjection experiments were next performed in epidermal cells of *N. benthamiana* sink (newly emerged leaves $<$ 1 cm long with immature block-shaped epidermal cells) and source (fully expanded leaves with jigsaw-shaped epidermal cells) leaves. Note that, in contrast to injection of mesophyll cells where the leaf epidermis is removed by peeling, injections of epidermal cells were performed with intact leaves. Neither OG-C4 nor OG-V1 exhibited extensive movement in epidermal cells of sink or source leaves, whereas extensive movement was observed for BDMV BC1 (Table 2). However, a higher frequency of LTAC movement was observed for V1 or C4 when injected into epidermal cells of sink (42% of injections for OG-C4 and 47% of injections for OG-V1) compared with source leaves (13% of injections for OG-C4 and OG-V1) (Table 2).

To determine whether the failure to observe extensive cell-to-cell movement of the TYLCV proteins was due to a need for an interaction between one or more viral proteins, various combinations of the OG-labeled TYLCV proteins were coinjected into *N. benthamiana* and tomato mesophyll cells. In none of the possible combinations was extensive cell-to-cell movement observed in mesophyll or epidermal cells of *N. benthamiana* sink and source leaves (Tables 1 and 2). In mesophyll cells, LTAC movement for the various combinations was generally similar to that observed for the individual proteins (Table 1). In epidermal cells of *N. benthamiana* sink leaves, coinjection of V1 and C4 resulted in a higher level of LTAC movement (80% of injections) compared with injections performed with either protein (~45% of injections) (Table 2).

The capacity of C4 and V1 to increase the PD SEL was next examined. Coinjection of 4-kDa F-dextran with unlabeled C4 or V1 protein into mesophyll cells of *N. benthamiana* and tomato leaves resulted in LTAC movement similar to that observed for the OG-labeled proteins. The F-dextran generally remained in injected cells (~80% of injections), whereas LTAC movement occurred in ~20% of injections (Table 1). Coinjection of various combinations of unlabeled proteins, together with 4-kDa F-dextran, revealed a pattern of LTAC movement that was similar to that observed with individual proteins, although the highest level of LTAC movement was observed with coinjection of V1 and C4 (Table 1). In control experiments, the BDMV BC1 mediated extensive cell-to-cell movement of the 4-kDa F-dextran in mesophyll cells

FIG. 1. Movement protein properties of fluorescently labeled *E. coli* expressed TYLCV and BDMV proteins in *N. benthamiana* mesophyll cells. (A) SDS–PAGE analysis showing *E. coli* expressed TYLCV V1, CP, C4, and BDMV BV1 and BC1 proteins. Control: protein profile for *E. coli* transformed with pRSETA alone. (B) to (G) Microinjection of TYLCV and BDMV OG-labeled proteins into *N. benthamiana* mesophyll cells. All images were collected 20 min after the fluorescent probe was introduced into the target cell except for (F), which was collected 5 min after injection. To illustrate the spatial relationship between the injected cell and the surrounding mesophyll, images were simultaneously collected in the FITC and red chlorophyll autofluorescence channels; four optically stacked sections were combined to generate the images presented. Asterisks in (B), (C), (D), and (G) indicate the injected cell. Bar in (B) is common to (C), (D), and (G). (B) TYLCV OG-C4 showing cell-to-cell movement limited to the cell(s) adjacent to the injected cell (LTAC movement). (C) TYLCV OG-V1 (LTAC movement). (D) BDMV OG-BC1 (extensive cell-to-cell movement). (E and F) Accumulation of TYLCV OG-CP in the nucleus; 5 min (E) and 20 min (F) after injection. In some cases, the signal accumulated at the periphery of the nucleus (inset). (G) Coinjection of unlabeled V1 and C4 facilitated LTAC movement of TOTO-1 labeled ds-DNA. Arrows indicate nuclei in which label (fluorescent DNA) had accumulated.

FIG. 2. Subcellular localization of TYLCV and BDMV GFP fusion proteins in *N. tabacum* protoplasts. (A) Construct used for transient expression of MP:GFP fusions. (B) to (M) Subcellular localization of MP:GFP constructs in *N. tabacum* protoplasts, 18–24 h posttransfection. Serial sections through protoplasts were obtained by CLSM. Bar = 10 μm. (B) Free GFP. (C) and (D) TYLCV V1-GFP showing distribution around (but not inside) the nucleus and in association with cytoplasmic strands and the cell periphery (C), or in association with punctate bodies in the cell cytoplasm (D). (E) and (F) ΔNV1-GFP (E) and ΔCV1-GFP (F) mutants. (G) Merging patterns of green fluorescence associated with V1-GFP and red fluorescence of the ER stain, rhodamine B-hexyl ester, showing colocalization with the ER. (H) TYLCV C4-GFP showing localization to the cell periphery. (I) and (J) ΔCC4-GFP (I) ΔNC4-GFP (J) mutants. (K) TYLCV CP-GFP showing accumulation in the nucleus and nucleolus. (L) and (M) ΔCCP-GFP (L) and ΔNCP-GFP (M) mutants. (N–P) BDMV BC1-GFP showing localization to the cell periphery (N), punctate bodies in the cell cytoplasm (O), and fibrous structures in the cytoplasm (P). (Q) BDMV BV1-GFP.

TABLE 1

Movement Protein Properties of TYLCV C4, V1, and Capsid Protein (CP) in *Nicotiana benthamiana* and Tomato Mesophyll Cells

Injected agent[a]	Coinjected agent	*N. benthamiana*		Tomato	
Lucifer yellow	—	57 (57)	(100.0%)	43 (43)	(100.0%)
3 kDa F-dextran	—	2 (61)[c]	(3.2%)	2 (40)[c]	(5.0%)
4 kDa F-dextran	—	1 (50)[c]	(2.0%)	1 (36)[c]	(2.7%)
10 kDa F-dextran	—	0 (42)[c]	(0%)	1 (53)[c]	(1.8%)
OG-BC1	—	28 (28)[b]	(100.0%)	15 (18)[b]	(83.0%)
OG-C4	—	7 (35)[c]	(20.0%)	5 (24)[c]	(21.0%)
OG-V1	—	8 (32)[c]	(25.0%)	7 (25)[c]	(28.0%)
OG-CP	—	1 (28)[c]	(3.6%)	0 (18)	(0%)
BC1	4 kDa F-dextran	21 (21)[b]	(100.0%)	12 (15)[b]	(80.0%)
C4	4 kDa F-dextran	6 (45)[c]	(13.0%)	11 (52)[c]	(21.0%)
V1	4 kDa F-dextran	9 (32)[c]	(28.0%)	6 (26)[c]	(23.0%)
CP	4 kDa F-dextran	0 (21)[c]	(0%)	1 (25)[c]	(4.0%)
OG-C4 + OG-V1	—	9 (29)[c]	(31.0%)	8 (25)[c]	(32.0%)
OG-C4 + OG-CP	—	4 (22)[c]	(18.0%)	6 (25)[c]	(24.0%)
OG-V1 + OG-CP	—	3 (20)[c]	(15.0%)	3 (18)[c]	(17.0%)
OG-(C4 + V1 + CP)	—	5 (23)[c]	(22.0%)	4 (18)[c]	(22.0%)
C4 + V1	4 kDa F-dextran	6 (25)[c]	(24.0%)	6 (20)[c]	(30.0%)
C4 + CP	4 kDa F-dextran	4 (23)[c]	(17.0%)	3 (22)[c]	(14.0%)
V1 + CP	4 kDa F-dextran	2 (20)[c]	(10.0%)	2 (21)[c]	(10.0%)
C4 + V1 + CP	4 kDa F-dextran	3 (22)[c]	(14.0%)	5 (20)[c]	(25.0%)
OG-C4 + OG-V1	TYLCV DNA	2 (20)[c]	(10.0%)	2 (15)[c]	(13.0%)
OG-C4 + OG-CP	TYLCV DNA	6 (20)[c]	(30.0%)	4 (15)[c]	(27.0%)
OG-V1 + OG-CP	TYLCV DNA	8 (22)[c]	(36.0%)	4 (15)[c]	(27.0%)
OG-(C4 + V1 + CP)	TYLCV DNA	2 (20)[c]	(10.0%)	5 (15)[c]	(33.0%)
ds-DNA-TOTO	—	0 (14)	(0%)	0 (15)	(0%)
ss-DNA-TOTO	—	0 (12)	(0%)	0 (10)	(0%)
ds-DNA-TOTO	CP	0 (12)	(0%)	0 (10)	(0%)
ds-DNA-TOTO	V1	1 (12)[c]	(8%)	1 (10)[c]	(10%)
ds-DNA-TOTO	C4	2 (12)[c]	(17%)	2 (10)[c]	(20%)
ss-DNA-TOTO	CP	0 (10)	(0%)	0 (10)	(0%)
ss-DNA-TOTO	V1	1 (10)[c]	(10%)	1 (10)[c]	(10%)
ss-DNA-TOTO	C4	2 (10)[c]	(20%)	1 (10)[c]	(10%)

[a] For description of TYLCV proteins, see Materials and Methods.

[b] Results are presented as number of injections in which extensive movement to neighboring cells (i.e., 8–15 cells beyond the injected cell) was observed/total number of injections, and the percentage in which such movement was observed.

[c] When movement was detected for TYLCV proteins, the fluorescent signal was detected only in cells adjacent to the injected cell (i.e., limited to adjacent cell movement, LTAC). These data are presented as injections in which LTAC movement occurred/total number of injections, as well as the percentage of injections in which such movement was observed.

of *N. benthamiana* (100% of injections) and tomato (80% of injections) (Table 1).

The need for DNA to form a protein–DNA complex competent for efficient cell-to-cell movement was tested by injecting unlabeled ss- or ds-DNA with the various OG-labeled protein combinations. As the results were similar to those obtained in the absence of DNA (Table 1), the LTAC pattern of movement was not attributable to a requirement for DNA to form a movement complex. Finally, the capacity of C4, V1, and CP to mediate cell-to-cell movement of fluorescently labeled ss- and ds-DNA was examined. When injected alone or with CP, neither ss- nor ds-DNA moved cell to cell (Table 1). When injected with V1 or C4, LTAC movement of fluorescently labeled ss- and ds-DNA was observed in 8–20% of the injections. In control injections, BC1 mediated extensive cell-to-cell movement of fluorescently labeled ss- and ds-DNA (data not shown).

TYLCV CP and C1 accumulate in the nucleus

A parallel set of microinjection experiments was performed with OG-labeled CP (OG-CP) and OG-labeled TYLCV C1, the replication-associated protein (OG-Rep; also expressed in *E. coli*, data not shown). The OG-CP failed to move cell to cell or mediate cell-to-cell movement of the 4-kDa F-dextran in mesophyll cells of tomato or *N. benthamiana* (Table 1). Similar results were obtained with OG-Rep (data not shown). Rather, in 46% of the injections, OG-CP accumulated within the nucleus of injected tomato and *N. benthamiana* mesophyll cells. Within 30 s after injection, fluorescent signal began to accumulate in the nucleus and nucleolus. The signal

TABLE 2

Cell-to-Cell Movement Properties of TYLCV C4 and V1 Proteins in *Nicotiana benthamiana* Epidermal Cells

Injected agent	Coinjected agent	Source	Sink
Lucifer yellow	—	12 (15)[a] (80%)	15 (15)[a] (100%)
4 kDa F-dextran	—	0 (15) (0%)	0 (12)[b] (0%)
10 kDa F-dextran	—	0 (12) (0%)	0 (15)[b] (0%)
OG-BC1	—	11 (12)[a] (92%)	12 (12)[a] (100%)
OG-C4	—	2 (15)[b] (13%)	5 (12)[b] (42%)
OG-V1	—	1 (15)[b] (13%)	7 (15)[b] (47%)
OG-V1	C4	2 (14)[b] (14%)	12 (15)[b] (80%)
C4 + V1	4 kDa F-dextran	2 (15)[b] (13%)	10 (13)[b] (77%)

[a] Results are presented as number of injections in which extensive movement to neighboring cells (i.e., 8–15 cells beyond the injected cell) was observed/total number of injections, and the percentage in which such movement was observed.

[b] Results are presented as number of injections in which the fluorescence was detected in cells adjacent to the injected cell. This is presented as injections in which movement occurred/total number of injections, as well as the percentage of injections in which such movement was observed.

then appeared to fluctuate between the nucleus and cytoplasm until, approximately 5 min after injection, the fluorescent signal began to accumulate in the nucleus (Fig. 1E). In some nuclei in which OG-CP accumulated, higher levels of fluorescence were observed at the periphery of the nucleus (Fig. 1F) and in the nucleolus, whereas in other cases the signal appeared to be evenly distributed throughout the nucleus and nucleolus. These results suggest that OG-CP can shuttle across the nuclear pore complex. The OG-Rep also accumulated in nuclei of *N. benthamiana* mesophyll cells (14 of 14 injections), consistent with its nuclear localization (Nagar *et al.,* 1995). In all of these experiments, the location of the nucleus within selected injected cells was confirmed using DAPI as described by Rojas *et al.* (1997).

Subcellular localization of the TYLCV and BDMV GFP fusion proteins in protoplasts and plant cells

To gain further insight into their role in TYLCV movement, the CP, V1, and C4 ORFs were individually fused, at the 3′ end, to the jellyfish green fluorescent protein (*GFP*) gene and placed under transcriptional control of the 35S promoter, to generate pCP-GFP, pV1-GFP, and pC4-GFP (Fig. 2A). These constructs were individually transfected into *Nicotiana tabacum* protoplasts to allow transient expression of the TYLCV–GFP fusion protein. Similar constructs also were generated for N- and C-terminal CP, V1, and C4 ORF deletion mutants. For all constructs, protoplasts were observed for GFP fluorescence at 18, 24, and 48 h posttransfection (hpt) with a confocal laser scanning microscope (CLSM). By 18 hpt, protoplasts transfected with a p35S-GFP construct showed extensive GFP fluorescence (signal) that was distributed throughout the cytoplasm, often in association with cytoplasmic strands, as well as in the nucleus (but not in the nucleolus) (Fig. 2B).

In most protoplasts transfected with pV1-GFP (70–80%), GFP fluorescence was distributed around the nucleus (perinuclear), in association with cytoplasmic strands, and at the cell periphery (Fig. 2C). CLSM analysis established that signal was not present inside the nucleus. In other cases (~20–30%), V1-GFP was associated with punctate bodies that were distributed throughout the cytoplasm (Fig. 2D). Protoplasts transfected with pΔNV1-GFP or pΔCV1-GFP did not exhibit a perinuclear pattern of GFP fluorescence or punctate bodies. Rather, signal was distributed throughout the cytoplasm and in the nucleus (Figs. 2E and 2F), similar to free GFP. These results suggested a role for the N- and C-termini in the subcellular localization of the V1 protein.

To determine whether the V1 protein was colocalized with the ER, protoplasts transfected with pV1-GFP were stained with the fluorescent lipophilic probe, rhodamine B hexyl ester, which labels endomembranes such as those of the ER system (Grabski *et al.,* 1993). In protoplasts expressing V1-GFP and stained with rhodamine B hexyl ester, a yellow-orange fluorescent signal was detected around the nucleus, on cytoplasmic strands, and at the cell periphery (Fig. 2G), suggesting colocalization of V1-GFP and the ER. Control protoplasts stained with rhodamine B hexyl ester showed a similar pattern of red fluorescence (data not shown). These results suggested that the TYLCV V1 interacts with ER network, from the perinuclear region out to the cell periphery.

In protoplasts transfected with pC4-GFP, GFP fluorescence was consistently observed at the cell periphery (Fig. 2H), suggesting an association of C4 with the plasma membrane. Protoplasts transfected with pΔCC4-GFP also exhibited signal localized to the cell periphery (Fig. 2I), whereas those transfected with pΔNC4-GFP showed signal in the cytoplasm and the nucleus, similar to free GFP. A computer-assisted functional domain search of the C4 amino acid sequence revealed an N-terminal myristoylation site [consensus sequence: GXXXS/T; Towler *et al.,* 1988; TYLCV C4 sequence: GNHIS] located within the 18 amino acids deleted in the ΔN-C4 mutant. N-terminal myristoylation domains are involved in membrane localization and protein–protein interactions, and many structural and nonstructural proteins of mammalian viruses are known to be N-myristoylated (Towler *et al.,* 1988; Johnson *et al.,* 1994). Together, these results suggested that C4 is a plasma membrane-associated protein and that a putative N-terminal myristoylation domain may play a role in membrane localization.

Protoplasts transfected with pCP-GFP exhibited GFP fluorescence inside nuclei and nucleoli, with little or no signal detected in the cytoplasm or at the cell periphery (Fig. 2K). With the pΔNCP-GFP and pΔCCP-GFP, signal was detected in nuclei but not nucleoli, and weak signal

TABLE 3

Cell-to-Cell Movement Properties of TYLCV V1- and C4-GFP Fusion Proteins in Epidermal Cells of *Nicotiana benthamiana* Leaves or Bean Hypocotyls

	Detached leaves[a]		Intact plants[b]		
	Sink	Source	Sink	Source	Bean hypocotyls
GFP	27 (396)[c] (6.8%)[d]	2 (131) (1.5%)	23 (247) (9.3%)	0 (129) (0%)	10 (194) (5%)
V1	71 (1111) (6.4%)	1 (413) (0.2%)	31 (329) (9.4%)	1 (280) (0.4%)	18 (356) (5%)
C4	21 (465) (5.4%)	2 (302) (0.7%)	14 (229) (6.1%)	3 (305) (1.0%)	9 (365) (3%)

[a] Source and sink leaves of 1-month-old *N. benthamiana* plants were detached and incubated in a Petri dish with moistened filter paper before bombardment.

[b] One-month-old *N. benthamiana* plants were bombarded, and source and sink leaves were detached prior to examination for GFP fluorescence with CLSM.

[c] Results are presented as number of bombardments in which movement to an adjacent cell(s) was observed/total number of bombarded cells expressing GFP.

[d] Percentage of bombardments in which movement into adjacent cells was observed.

also was detected within the cytoplasm and at the cell periphery (Figs. 2L and 2M). These results suggested that the N- and C-terminal regions of the CP may play a role in the targeting of the CP within nuclei, but that these regions are not essential for nuclear localization of the CP–GFP fusion proteins. Nuclear localization of the CP–GFP in protoplasts was consistent with microinjection results showing CP accumulation in the nucleus and nucleolus.

To compare patterns of intracellular localization of the TYLCV C4, V1, and CP with those of the BC1 and BV1 MPs of a bipartite begomovirus, the *GFP* gene was fused to the 3′ end of the BDMV BV1 and BC1 ORFs to generate pBV1-GFP and pBC1-GFP, respectively (Fig. 2A). Protoplasts transfected with pBC1-GFP exhibited three different patterns of GFP fluorescence: (i) signal predominantly localized to the cell periphery (Fig. 2N), (ii) signal localized to punctate bodies (Fig. 2O), and (iii) signal localized to fibrous structures (Fig. 2P). Importantly, no tubule-like structures, such as those that have been described for viruses thought to move cell to cell as virions (e.g., Kasteel *et al.,* 1996), were observed on protoplasts transfected with pBC1-GFP or any other construct. Protoplasts transfected with pBV1-GFP showed fluorescence inside nuclei and nucleoli (Fig. 2Q). These results are consistent with the previously established role of BDMV BV1 in mediating nuclear export of viral DNA and BC1 in facilitating cell-to-cell movement of viral DNA through PD (Noueiry *et al.,* 1994; Rojas *et al.,* 1998).

We next evaluated the subcellular localization of the V1-, C4-, and CP-GFP fusion proteins in *N. benthamiana* epidermal cells, and the capacity of any of these proteins to move cell to cell in these tissues. The p35S-GFP, pC4-GFP, pV1-GFP, and pCP-GFP constructs were indi-

FIG. 3. Movement protein properties of TYLCV GFP fusion proteins transiently expressed in epidermal cells of *N. benthamiana* sink and source leaves and bean hypocotyls. Transient expression constructs (Fig. 2A) for TYLCV C4-, V1-, and CP-GFP were introduced into epidermal cells of *N. benthamiana* leaves or bean hypocotyls by particle bombardment. Images were collected with a CLSM 24 h postbombardment. Bar = 10 μm. Images (A), (D), and (G); (B), (E), and (H); (C), (F), and (I); and (J) and (K) were taken at the same magnification. (A) to (C) Free GFP in epidermal cells of bean hypocotyls (A) and *N. benthamiana* source (B) and sink (C) leaves. Movement of free GFP into cells adjacent to the bombarded cell (C). (D) to (F) TYLCV V1-GFP showing distribution around the nucleus and in association with cytoplasmic strands and the cell periphery of epidermal cells of bean hypocotyls (D) and *N. benthamiana* source (E) and sink (F) leaves. Movement of V1-GFP into cells adjacent to the bombarded cell (F). (G) to (I) TYLCV C4-GFP showing localization to the cell periphery in epidermal cells of bean hypocotyls (G) and *N. benthamiana* source (H) and sink (I) leaves. (J) and (K) TYLCV CP-GFP showing accumulation in the nucleus and nucleolus of epidermal cells of bean hypocotyls (J) and *N. benthamiana* sink (K) leaves.

FIG. 4. Localization of TYLCV in infected tomato plants. Sections were prepared from TYLCV-infected tissues collected from plants at different stages of growth. Images were collected with a phase contrast light microscope. Bar = 100 μm; images (A), (B), (D), (E), (G), (H), and (I); (C) and (F); (J) and (K); and (L) and (M) were taken at the same magnification. (A) Stem section of an uninfected tomato plant probed with TYLCV CP antiserum. (B) Stem section from a TYLCV-infected tomato plant probed with CP antiserum and showing signal over cells of the internal and external phloem. (C) Higher magnification of the vascular cells of (B) showing signal over companion cells and sieve elements. (D) Section of a mature leaf from an uninfected plant probed with TYLCV C4 antiserum. (E) and (F) Section of a mature leaf from a TYLCV-infected plant probed with C4 antiserum and showing signal over the cells of the internal and external phloem. (G) Section of a young leaf from an uninfected plant probed with CP antiserum. (H) and (I) Sections of young leaves from TYLCV-infected plants probed with CP antiserum. (J) Section of a shoot apex from an uninfected plant probed with CP antiserum. (K) Section of a shoot apex from a TYLCV-infected plant probed with CP antiserum and showing signal over the developing cells of the phloem. Arrows indicate the developing internal and external phloem tissues. (L) Stem section of an uninfected tomato plant from *in situ* PCR experiments. (M) Stem section of a TYLCV-infected tomato plant showing signal over the nuclei of phloem-associated cells in *in situ* PCR experiments. Arrows indicate labeled nuclei. Abbreviations: cc = companion cells; ip = internal phloem, ep = external phloem, se = sieve element, x = xylem.

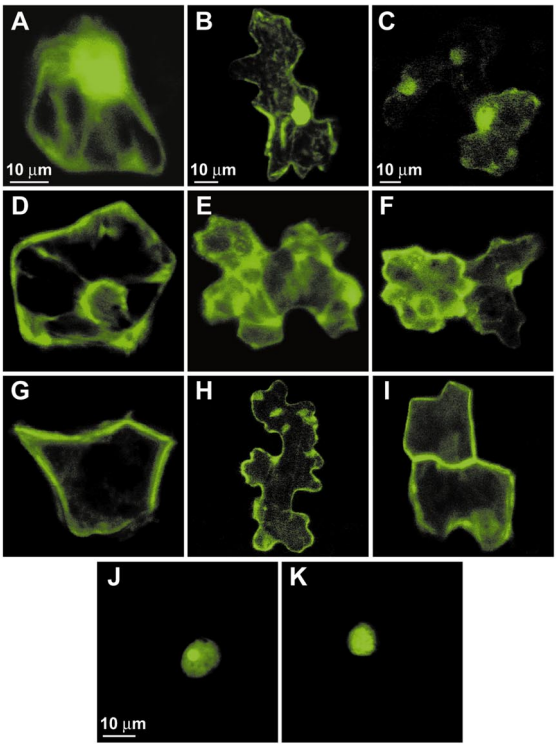
A
B
C
10 µm
10 µm
10 µm
D
E
F
G
H
I
J
K
10 µm

3

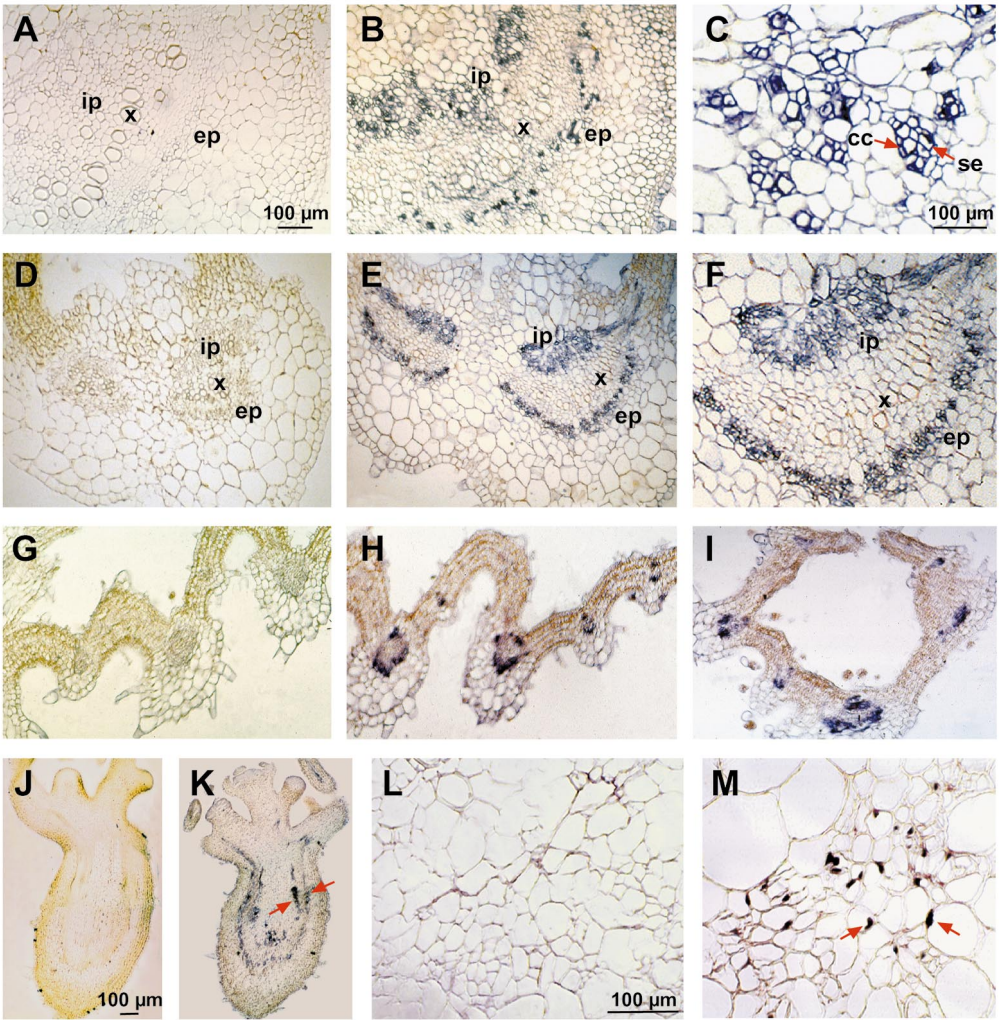
A
ip
x
ep
100 µm
B
ip
x
ep
C
cc
se
100 µm
D
ip
x
ep
E
ip
x
ep
F
ip
x
ep
G
H
I
J
100 µm
K
L
100 µm
M

4

vidually bombarded into epidermal cells of detached and attached *N. benthamiana* sink and source leaves and hypocotyls of 3-day-old bean seedlings. Bombarded tissues were examined for GFP fluorescence 24 and 48 h postbombardment (hpb). Irrespective of the construct tested, similar results were obtained for detached vs attached leaves (Table 3). At 24 hpb, free GFP was detected in the cytoplasm and nucleus of bombarded epidermal cells of *N. benthamiana* leaves and bean hypocotyls, and a similar pattern was observed 48 hpb (Figs. 3A and 3B). However, in a few cases, GFP fluorescence was detected in foci of two to three epidermal cells (Fig. 3C). The highest proportion of these foci were observed in epidermal cells *N. benthamiana* sink leaves (7–9% of bombardments), followed by bean hypocotyls (5% of bombardments), and *N. benthamiana* source leaves (0–1.5% of bombardments) (Table 3).

Epidermal cells bombarded with pV1-GFP showed GFP fluorescence around the nucleus and in association with cytoplasmic strands that extended to the cell periphery (Figs. 3D–3F). In some cases, cells showed punctate fluorescent bodies in the cytoplasm and at the cell periphery. These subcellular localization patterns were similar to those observed for V1-GFP in protoplasts. By 48 hpb, GFP fluorescence was usually confined (>90% of bombardments) to individual epidermal cells of bombarded leaf and hypocotyl tissue. Occasionally, signal was detected in foci of two to three cells (Fig. 3F), with the proportion of such foci being greatest in *N. benthamiana* sink leaves (6–9% of bombardments), followed by bean hypocotyls (5% of bombardments) and *N. benthamiana* source leaves (0.2–0.4% of bombardments) (Table 3). These results indicated that V1-GFP has a limited capacity for cell-to-cell movement in epidermal cells of sink or source leaves.

Equivalent experiments conducted with pC4-GFP revealed GFP fluorescence accumulated at the cell periphery (Figs. 3G–3I), similar to the subcellular localization pattern observed for C4-GFP in protoplasts. By 48 hpb, GFP fluorescence was usually confined to individual cells (94% of bombardments), regardless of the tissue type. In bombarded sink leaves, foci of two cells were occasionally observed (5–6% of bombardments), whereas these foci were less commonly observed in bean hypocotyls (3% of bombardments) and *N. benthamiana* source leaves (1% of bombardments) (Table 3 and Fig. 3I).

In epidermal cells bombarded with pCP-GFP, GFP fluorescence was confined to individual bombarded cells and signal accumulated in nuclei and nucleoli (Figs. 3J and 3K). These results are also consistent with those obtained in protoplast experiments, although visualization of CP–GFP fluorescence was more difficult in epidermal cells than with protoplasts.

TYLCV CP mediates nuclear import and export of DNA

Microinjection and transient expression experiments revealed that the TYLCV CP enters and accumulates in the nucleus and nucleolus. Moreover, as neither C4 nor V1 showed any nuclear accumulation, these results suggested that the TYLCV CP serves as a nuclear shuttle protein, in a manner similar to that of BV1 for the bipartite begomoviruses (e.g., BDMV). To investigate whether the CP mediates export of DNA from the nucleus, double microinjection experiments were performed. Here, circular ss-DNA (M13 mp18) or circular ds-DNA (pTY-DR1), labeled with TOTO-1, were first injected into *N. benthamiana* mesophyll cells. In these injections, fluorescently labeled DNA (ss- and ds-DNA) remained within the injected cell and, within 5 min, fluorescence began to concentrate in the nucleus. Approximately 15 to 20 min after injection, the fluorescence had concentrated in the nucleus and nucleolus (Table 4), where it remained for as long as 1 h after injection (the duration of these experiments). The identity of nuclei was confirmed by DAPI staining.

In the next series of experiments, fluorescently labeled DNA was allowed to accumulate in the nucleus/nucleolus of the injected cell and, then, a second injection was used to introduce unlabeled CP. Such cells were then observed for dissipation of the fluorescence from the

TABLE 4

Nucleocytoplasmic Transport of DNA Mediated by TYLCV Capsid Protein (CP) in *N. benthamiana* Mesophyll Cells

First injected agent[a]	Nuclear accumulation of fluorescent probe[b]	Second injected agent	Nuclear export of DNA[c]
ds-DNA-TOTO	9 (10)	—	0 (9)
ss-DNA-TOTO	10 (10)	—	0 (10)
ds-DNA-TOTO	10 (12)	BV1	7 (10)
ds-DNA-TOTO	24 (28)	CP	11 (24)
ds-DNA-TOTO	11 (12)	V1	2 (11)
ds-DNA-TOTO	12 (12)	C4	0 (12)
ss-DNA-TOTO	10 (10)	BV1	7 (10)
ss-DNA-TOTO	24 (25)	CP	15 (24)
ss-DNA-TOTO	10 (10)	V1	0 (10)
ss-DNA-TOTO	9 (10)	C4	0 (9)

[a] pTY1-DR (50 ng/μl) was used as ds-DNA and M13 mp8 (100 ng/μl) was used as ss-DNA.

[b] Results presented represents the number of injections in which fluorescence accumulated in nuclei and nucleoli of injected cells 20 min after injection/total number of injections performed. The identity of nuclei was confirmed using DAPI stain.

[c] A positive result for nuclear export was recorded when at least 50% of the fluorescence that had accumulated in the nucleus had moved into the cytoplasm and the perinuclear region. In all cases where nuclear export was recorded, fluorescence was no longer observed in the nucleolus. Observations were made over a 20-min period after injection of the second agent.

TABLE 5

Nucleocytoplasmic Transport of DNA Mediated by TYLCV CP Is Enhanced by V1

First injected agent[a]	Nuclear accumulation of fluorescent probe[b]	Second injected agent	Nuclear export of DNA[c]	Third injected agent	Nuclear export of DNA[c]	Cell-to-cell movement (LTAC)[d]
ds-DNA-TOTO[a]	15 (18) (83%)	CP	7 (15)[b] (46%)	V1	10 (15)[b] (66%)	0 (18)[c] (0%)
ds-DNA-TOTO	10 (12) (83%)	CP	4 (10) (40%)	V1+C4	7 (10) (70%)	4 (10) (40%)
ds-DNA-TOTO	8 (10) (80%)	CP	3 (8) (38%)	C4	3 (8) (38%)	2 (8) (25%)
ds-DNA-TOTO	12 (15) (80%)	CP+V1	9 (12) (75%)	C4	9 (12) (75%)	4 (12) (33%)
ds-DNA-TOTO	9 (10) (90%)	CP+C4	4 (9) (44%)	—	—	2 (9) (22%)

[a] pTY1-DR (50 ng/μl) was labeled with TOTO-1-iodine.

[b] Results presented represent the number of injections in which fluorescence accumulated in nuclei of injected cells 15 to 20 min after injection/total number of injections performed. The identity of nuclei was confirmed using DAPI stain.

[c] A positive result for nuclear export was recorded when at least 50% of the fluorescence that had accumulated in the nucleus had moved into the cytoplasm and the perinuclear region. In all cases where nuclear export was recorded, fluorescence was no longer observed in the nucleolus. Observations were made over a 20-min period after injection of the third agent.

[d] Results are presented as number of injections in which fluorescence was detected in cells adjacent to the injected cell.

nucleus, i.e., CP-mediated nuclear export of labeled DNA. Based on these experiments, the CP mediated nuclear export of DNA in a two-step process. In the first step, observed in all injections, fluorescence dissipated from the nucleolus and concentrated at the periphery of the nucleus. This pattern of fluorescence was similar to that sometimes observed for OG-CP in microinjection studies (Fig. 1F). In the second step, fluorescence dissipated from the periphery of the nucleus into the cytoplasm immediately surrounding the nucleus. The TYLCV CP mediated the export of ss-DNA and ds-DNA, as did BDMV BV1 (Table 4). In equivalent experiments, V1 and C4 did not mediate nuclear export of DNA.

We next tested whether CP influenced accumulation of ss- or ds-DNA in the nucleus. In these experiments, fluorescently labeled ss- or ds-DNA was mixed with unlabeled CP and then injected into *N. benthamiana* mesophyll cells. In the presence of CP, fluorescence accumulated in nuclei in all injections, and the rate of accumulation was enhanced compared with DNA alone (e.g., 5 min for complete accumulation with CP vs 15–20 min for accumulation of DNA alone). Interestingly, in these experiments, nuclear export was infrequently observed (<10% of injections), suggesting that export may be a sequential process that first requires nuclear accumulation of DNA. In equivalent experiments, DNA accumulated in the nucleus and nucleolus in the presence of V1 or C4, but the rate of DNA accumulation was not enhanced (data not shown).

TYLCV V1 enhanced the capacity of CP to mediate nuclear export of DNA

Nuclear export of DNA, mediated by the CP, often resulted in a perinuclear distribution of fluorescently labeled DNA. As the V1-GFP also showed a perinuclear distribution, we next tested whether V1 influenced the capacity of the CP to mediate DNA export into the cytoplasm. In these experiments, fluorescently labeled ds-DNA was injected and allowed to accumulate within the nucleus. Next, the CP was injected into these cells and nuclear export was recorded. Consistent with previous results, nuclear export was observed in 43% of such injections (Table 5). A third injection was then employed to introduce V1, C4, or V1 and C4 into such cells. In the presence of V1 or V1 and C4, nuclear export of DNA was enhanced by 20–30%, whereas C4 alone did not enhance export (Table 5). A similar enhancement of DNA export was observed when CP and V1 were coinjected (second injection). These results suggested that V1 plays a role in nuclear export, possibly via an interaction with a CP–DNA complex. Although introduction of C4, as the third injection treatment, did not enhance nuclear export, the presence of C4 sometimes mediated the movement of fluorescently labeled DNA into adjacent cells (Fig. 1G; Table 5).

Immunolocalization of TYLCV in infected tomato plants

To determine the cell and tissue types infected by TYLCV, immunolocalization studies with CP and C4 antisera were conducted with tissues (stems, young and mature leaves, and shoot apices) collected from TYLCV-infected tomato plants at preflower, flowering, and fruit formation stages of growth. Controls consisted of equivalent tissues from uninfected plants probed with CP and C4 antisera, and infected and uninfected tissues probed with preimmune antisera. All such controls revealed an absence of immunolabeling (Figs. 4A, 4D, 4G, and 4J). In all infected tissue types examined, with either C4 or CP antisera, label was detected in association with vascular

tissues. Particularly strong labeling was observed over cells of the internal and external phloem of the stem and veins of young and mature leaves (Figs. 4B, 4C, 4E, 4F, 4H, and 4I). In stems and mature leaves, label appeared to be confined to SE, CC, and phloem parenchyma (PP) cells (Fig. 4C). Strong labeling was also detected over phloem cells of shoot apices (Fig. 4K) and flowers.

In situ PCR experiments, performed using a TYLCV primer pair that directed the amplification of an ~500-bp fragment of the C1 ORF, were conducted with tissue sections equivalent to those used in the immunolocalization studies. In preliminary PCR experiments, this primer pair directed the amplification of the expected 500-bp fragment from DNA extracts prepared from TYLCV-infected, but not uninfected, tomato tissues (data not shown). In stem sections of TYLCV-infected plants, TYLCV DNA was detected only in phloem tissues, with the strongest signal over the nuclei of phloem-associated cells (Fig. 4M) and cells of the developing CC–SE complex. No signal was detected from sections of uninfected tissues (Fig. 4L). *In situ* PCR experiments performed on young and mature leaf tissues revealed TYLCV DNA within nuclei of cells of the cambium and the phloem. In general, *in situ* PCR results were similar to those obtained by immunolocalization and, collectively, these results established that TYLCV is phloem-limited in tomato, irrespective of the organ or stage of plant growth examined.

DISCUSSION

The monopartite begomoviruses lack a DNA-B component as well as obvious BV1 and BC1 homologues. In the present study, we demonstrate that the TYLCV CP functions in the shuttling of DNA between the nucleoplasm and the cytoplasm and, therefore, acts as the homolog to the bipartite begomovirus BV1. However, none of the TYLCV proteins showed MP properties equivalent to those displayed by the bipartite BDMV BC1. Rather, both the TYLCV V1 and the C4 demonstrated a limited capacity to interact with PD to mediate an increase in SEL and effect cell-to-cell movement of DNA (i.e., LTAC movement). The potential biological relevance of this form of movement for TYLCV is suggested by the finding that delivery, via particle bombardment, of infectious TYLCV DNA into hypocotyl tissue of young bean seedlings resulted in the establishment of systemic infection (J. Potter and D. P. Maxwell, personal communication). This finding is consistent with a capacity for cell-to-cell movement in nonphloem cells of the bean hypocotyl (Sudarshana *et al.,* 1998). However, the relatively inefficient interaction between TYLCV proteins and epidermal and mesophyll PD may explain the phloem-limited nature of TYLCV infections in tomato. This was recently suggested to be the mechanism underlying phloem limitation of a bipartite begomovirus (Morra and Petty, 2000).

Interaction between TYLCV proteins and host cellular components

Microinjection and transient expression experiments provided insight into the mechanism by which the C4, V1, and CP may function in TYLCV movement. The CP localized to nuclei and nucleoli and was found to act as a nuclear shuttle, mediating the import and export of DNA (Fig. 1, Table 4). Thus, our findings are consistent with results obtained for the TYLCV CP in heterologous experimental systems (Kunik *et al.,* 1998; Rhee *et al.,* 2000). A similar situation was recently shown for the CP of the monopartite mastrevirus, *Maize streak virus* (MSV) (Liu *et al.,* 1999, 2001).

Nucleolar abnormalities have been observed in geminivirus-infected cells (Kim *et al.,* 1978; Cherif and Russo, 1983; Channarayappa *et al.,* 1992), but the biological significance of nucleolar localization is unknown. Interestingly, the TYLCV CP was found to accumulate in the nucleolus. The absence of the N- and C-terminal CP mutants from the nucleolus implicates CP motifs in this localization. As the nucleolus is the site of rRNA synthesis and packaging of ribosomal proteins, it may also serve as the site of geminiviral replication/gene expression.

Neither the V1 nor C4 accumulated in the nucleus. The V1 displayed a perinuclear distribution that extended to the cell periphery, and it was colocalized with the ER. MPs of a number of viruses have now been localized to the ER, including the TMV MP (Heinlein *et al.,* 1998), *Alfalfa mosaic virus* MP (Zheng *et al.,* 1997), and the SLCV BC1 (Ward *et al.,* 1997), suggesting that MP–ER interactions are important for intracellular and intercellular trafficking of the infectious form of the virus (Lazarowitz and Beachy, 1999).

Both the TYLCV C4 and the bipartite begomovirus BC1 are targeted to the cell periphery and/or cell wall, consistent with a role in cell-to-cell movement of viral DNA (Pascal *et al.,* 1993; Sanderfoot and Lazarowitz, 1995; von Arnim *et al.,* 1993). Our observation that coinjection of V1 and C4 led to an increased efficacy of LTAC movement (Table 2) suggests a role for V1 in this process. The C4 may mediate TYLCV movement by targeting a V1-TYLCV DNA complex to the cell periphery and presumably to the PD. Another feature shared between C4 and BC1 proteins is the capacity to induce disease symptoms when expressed in transgenic plants (Duan *et al.,* 1997; Hou *et al.,* 2000; Krake *et al.,* 1998; Latham *et al.,* 1997). Although the mechanism underlying this phenomenon is unknown, it may relate to the localization of the cell periphery, where these proteins may interfere with the trafficking of endogenous macromolecules (Hou *et al.,* 2000; Latham *et al.,* 1997).

Phloem tropism of TYLCV

The immunolocalization and *in situ* PCR results presented in this study provide strong support for the concept that TYLCV is phloem-limited in its natural host tomato. This finding is consistent with previous ultrastructural studies (Russo *et al.,* 1980; Cherif and Russo, 1983; Channarayappa *et al.,* 1992; but see Michelson *et al.,* 1997). Here, it is important to emphasize that TYLCV was confined to cells of the phloem in the shoot apical, developing leaf, stem, and floral tissues of tomato plants at three stages of growth (Fig. 4). The extensive labeling of phloem tissues in shoot apices and young leaves demonstrated the efficacy with which TYLCV can invade and replicate within these strong sink tissues. Equivalent patterns of infection have been observed for BDMV in *N. benthamiana* and bean plants (Wang *et al.,* 1996; Sudarshana *et al.,* 1998), and for the phloem-limited curtovirus, *Beet curly top virus*, in *N. benthamiana* (Latham *et al.,* 1997). Given that TYLCV does not egress into surrounding nonphloem cell types, a boundary at or near the vasculature must exist that blocks viral transport into these tissues. The nature of this boundary remains to be elucidated.

Recent studies have suggested that free GFP and proteins up to 50 kDa can move, extensively, cell to cell in sink but not source tissues, and this was correlated with a transition from primary to secondary PD (Oparka *et al.,* 1999). Thus, it was conceivable that the infectious form of TYLCV could move more efficiently through PD in sink tissues. Our microinjection and transient expression experiments failed to detect a capacity for extensive cell-to-cell movement in sink leaves, although the frequency of LTAC movement was higher in sink leaves. Thus, the movement of V1 or C4 in such tissues was not anywhere near the degree and extent reported by Oparka *et al.* (1999) for free GFP. Moreover, in our studies, movement of GFP in sink leaves was also found to be quite limited in extent (Table 3). Therefore, the limited capacity of the TYLCV V1 and C4 proteins to interact with epidermal and mesophyll PD in sink and source leaves is consistent with the phloem-limited nature of TYLCV.

Insight into the nature of the TYLCV phloem limitation may come from recent studies conducted with the monopartite MSV (Kotlitzky *et al.,* 2000). Here, the MSV V1 moved, cell to cell, in an LTAC pattern similar to that of TYLCV V1 but, importantly, it underwent extensive movement (>10 cells) in ~15–20% of bombarded maize cells. This difference in V1 movement between MSV and TYLCV may well reflect the fact that MSV is not phloem-limited in maize (Lucy *et al.,* 1996). The V1–host interaction that results in this more extensive movement may allow MSV to egress from the phloem.

As TYLCV is phloem-limited and does not encode MPs that efficiently interact with epidermal or mesophyll PD, it is possible that V1 and C4 may interact more efficiently with PD of phloem cells to mediate spread of the infectious form of the virus. For example, in the shoot apex, V1 and C4 could function, with or without phloem-associated host factors, to mediate cell-to-cell movement of viral DNA into and between developing phloem cells. Together with movement aided by cell division in this tissue (Latham *et al.,* 1997), this would allow for extensive infection of phloem progenitor cells and, subsequently, the mature phloem cells (e.g., CC and SE). Unfortunately, direct injection of proteins into nucleate phloem cells was not possible due to technical limitations. Therefore, direct experimental evidence for V1 and C4 function in phloem cells will have to come from other approaches, possibly by using transgenic plants expressing these proteins under the control of a phloem-specific promoter (Oparka and Turgeon, 1999).

A model for TYLCV movement

A role for virions in TYLCV cell-to-cell and/or long-distance movement can not be discounted. However, the experiments presented here addressed the capacity of the virus to move as a nucleoprotein complex and, thus, a model will be developed based on this premise. Following introduction of virions into the SE by whiteflies, the CP may enhance the uptake of viral DNA into nuclei of developing phloem cells in sink tissues. Once viral DNA has begun to replicate in the nucleus/nucleolus of a phloem cell, newly synthesized CP carries out at least two distinct functions: (i) nuclear export of the infectious form of the virus, and (ii) encapsidation of ss-DNA into virions. An intriguing possibility is that the CP mediates nuclear export of ds-DNA RF for cell-to-cell and long-distance movement within the plant and encapsidates ss-DNA within the nucleus to form virions that are required for plant-to-plant spread via the whitefly vector. At the nuclear periphery, V1 serves to enhance nuclear export of viral DNA and then it mediates the delivery of viral DNA to the cell periphery, possibly through an interaction with the ER. Here, C4, through a putative N-terminal myristoylation domain, acts in the delivery of the viral DNA to the PD and mediates cell-to-cell transport. Upon entry into an adjacent uninfected phloem cell, the viral DNA moves across the nuclear pore complex to repeat the infection cycle. To initiate a systemic infection, the viral DNA or virions must cross the specialized PD of the CC-SE to enter the SE for delivery to sink tissues (most critically the shoot apex).

It is clear from the perspectives of genome organization and functional properties revealed in various experimental systems that the TYLCV CP carries out function(s) performed by the bipartite begomovirus BV1. This is consistent with the concept that these proteins share a common evolutionary origin (Kikuno *et al.,* 1984). The situation with respect to the TYLCV V1 and C4 is less

obvious as the sequences and functional properties of these proteins differ substantially from previously studied MPs, including BC1 of the bipartite begomoviruses. These features may reflect the acquisition (from the host genome) and/or extensive modification (via parallel evolution) of sequences to generate a specialized MP system that interacts with the endogenous macromolecular trafficking machinery of the phloem to facilitate movement of the infectious form of the virus. Further resolution of the similarities and differences between cell-to-cell and long-distance movement of monopartite vs bipartite begomoviruses will require functional analysis of viral proteins in phloem cells and the identification of the form(s) in which these viruses move within the plant.

MATERIALS AND METHODS

Plant materials

N. benthamiana Domin. and *Lycopersicon esculentum* L. plants used in microinjection experiments were grown in a controlled environment chamber (Conviron Model PGR 15; Winnipeg, Manitoba) maintained at 25°C under 16 h photoperiod and irradiance levels of ~700–1000 μmol m^{-2} s^{-1}. Leaves from 4- to 5-week-old plants were used for microinjection experiments.

Cloning of TYLCV C4, V1, and CP ORFs for protein expression

The TYLCV C4, V1, and CP ORFs were amplified from pTY1-DR, a recombinant plasmid that contains a full-length infectious clone of TYLCV-DO (Nakhla *et al.,* 1994) by PCR (10 cycles of 94°C for 1 min, 55°C for 1 or 2 min, and 72°C for 2 or 3 min) with proofreading *Taq* polymerase (Vent; New England Biolabs, Beverly, MA). PCR primers were designed based upon the TYLCV-DO sequence (Salati, 2001), and *Bam*HI (5′) and *Pst*I (3′) sites were introduced to facilitate cloning into the protein expression vector, pRSET A (Invitrogen Corp., Carlsbad, CA). Following this approach, recombinant plasmids pC4, pV1, and pCP were generated for expression of TYLCV C4, V1, and CP, respectively, in *E. coli*. The integrity of the cloned TYLCV sequences in these plasmids was confirmed by sequencing.

Protein expression, purification, and labeling

Recombinant plasmids were transformed into *E. coli* strain JM 109:D3 and protein expression was induced as previously described (Noueiry *et al.,* 1994; Rojas *et al.,* 1997). *E. coli* expressed fusion proteins were further purified using Ni-NTA columns according to the manufacturer's instructions (Qiagen, Valencia, CA). Column-purified proteins were labeled with FITC-OG according to manufacturer's instructions (Molecular Probes, Eugene, OR) and renatured as previously described (Rojas *et al.,* 1997). The quantity and purity of proteins were determined by SDS–polyacrylamide gel electrophoresis and comparison to known quantities of protein standards.

Nucleic acid labeling

Circular ds-DNA (pTY1-DR, 5.8 kb) and ss-DNA (M13 mp18, 6.4 kb) were labeled with the fluorescent dye, TOTO-1-iodine, according to the manufacturer's instructions (Molecular Probes). Excess dye was removed by recovering labeled DNA with a purification kit (Qiagen).

Microinjection and confocal laser scanning imaging

Before and after microinjection, aliquots of FITC-OG-labeled proteins and TOTO-1-labeled DNA were examined by gel electrophoresis to confirm the integrity of the injected material (Rojas *et al.,* 1997). Microinjections were performed as described (Noueiry *et al.,* 1994). Movement of fluorescent probes within cells of tomato and *N. benthamiana* leaves was observed using a Leica upright CLSM (model TCS-4D; Leica, Heidelberg, Germany) equipped with a Narishige four-dimensional hydraulic micromanipulator system (Narishige, Tokyo, Japan). A low-intensity laser (25 mW krypton/argon laser) was used to image the spatial distribution of FITC-OG and TOTO-1. Simultaneous two- or three-channel recordings were made using the following filter sets: FITC-OG, 488-nm excitation, 525-nm emission; TOTO-1, 514-nm excitation, 533-nm emission; and chlorophyll autofluorescence, 488-nm excitation, 590-nm emission. All experiments were conducted and analyzed with the same laser power and photomultiplier settings. At the conclusion of each experiment, data files were transferred to a Power Mac 8500 workstation. Image analysis, display (adjustments in contrast, brightness, etc.), and preparation of figures were performed with Adobe Photoshop (Adobe Systems, Inc., Mountain View, CA).

Generation of plasmids for TYLCV and BDMV MP-GFP transient expression experiments

Full-length and 5′ and 3′ deleted forms of the TYLCV C4, V1, and CP ORFs were amplified from pTY1-DR, and full-length BDMV BV1 and BC1 ORFs were amplified from pBDB1 (Gilbertson *et al.,* 1991) by PCR as previously described (Rojas *et al.,* 1993) (primer sequences available upon request). The ΔNCP and ΔCCP mutants had 180 and 150 nt deleted, respectively. ΔNV1 and ΔCV1 mutants had 63 and 84 nt deleted, respectively; and ΔNC4 and ΔCC4 mutants had 54 and 60 nt deleted, respectively. Stop codons were removed to allow 3′ fusion with the *GFP* gene, and *Xba*I and *Nhe*I sites were added to the ends of the 5′ and 3′ primers, respectively, to facilitate cloning with the Zero Blunt PCR cloning kit (Invitrogen). After cloning each of the ORFs in the pCR-Blunt vector, the insert in selected recombinant plasmids was sequenced to confirm the integrity of each cloned ORF. Each ORF was then released by digestion with *Xba*I

and *Nhe*I and ligated into 35S-mGFP5 (M. R. Sudarshana, unpublished results), which places the expression of the MP-mGFP5 fusion protein under the control of the 35S promoter and the NOS terminator (Fig. 2A).

Transient expression assays with TYLCV C4-, V1-, and CP-GFP constructs

Protoplasts were prepared from *N. tabacum* cv. Xanthi nc cell suspension cultures as previously described (Hou *et al.,* 1998). For each construct, 10 μg DNA was electroporated into approximately 3×10^6 protoplasts (290 V, 490 μF for 8 ms). The transfected protoplasts were kept in the dark at room temperature and examined for GFP expression at 18, 24, and 48 hpt. To identify the ER, 10 μl rhodamine B hexyl ester (100 μg/ml in DMSO stock solution; Molecular Probes) was added to 1 ml of cells 18–24 hpt, cells were incubated for 5 min and then observed by CSLM.

For transient expression experiments in epidermal cells, attached and detached fully expanded (source) and young (sink) leaves of 1-month-old *N. benthamiana* plants (five-to-seven leaf stage) and hypocotyls of 3-day-old bean seedlings (cv. Topcrop) were used. Detached leaves were placed into Petri dishes containing moistened filter paper. The adaxial surface of *N. benthamiana* leaves and the surface of bean hypocotyl tissues were bombarded (1550 psi; PDS-1000 particle acceleration device; DuPont, Wilmington, DE) with gold particles coated with the appropriate MP-GFP expression plasmids. Leaves were maintained at 25°C until observation for GFP fluorescence with the CLSM.

Tissue fixation and immunolocalization

Stem, leaf (young and mature), and shoot apex tissues (vegetative and floral) were excised from uninfected and TYLCV-infected tomato plants. All tissue samples were fixed, dehydrated, and paraffin-embedded according to the methods described by Smith *et al.* (1992) and modified in Jackson *et al.* (1994). Paraffin-embedded tissues were sectioned (10 μm; model HM340E microtome, Microm, Walldorf, Germany) and rehydrated prior to incubation with antisera.

To produce antisera, the *E. coli* expressed TYLCV CP fusion protein was fractionated by SDS–PAGE. Gels were stained with Coomassie brilliant blue R-250 (Bio-Rad Laboratories, Hercules, CA) and the protein band corresponding to the CP fusion protein (34 kDa) was excised and macerated in 2 ml Freund's incomplete adjuvant. The protein preparation was injected into New Zealand giant rabbits by Antibodies Inc. (Davis, CA). Preimmune antiserum was obtained from each rabbit before immunization. The C4 antisera was generated by Genosys Biotechnologies (The Woodland, TX) using an oligopeptide (SRPTWRKTETSLILE) predicted to represent an antigenic region of the protein. The peptide was conjugated to bovine serum albumin (BSA), purified, and used to produce polyclonal antisera in rabbits.

Detection of TYLCV CP and C4 was carried out on fixed tissue using the methods described by Smith *et al.* (1992) as modified by Jackson *et al.* (1994). The CP and C4 antibodies were used in dilutions of 1:500 and 1:1000, respectively, and were detected by goat anti-rabbit antibodies conjugated to alkaline phosphatase (AP) that was diluted 1:2000. AP activity was measured with nitroblue tetrazolium (NBT) and bromo-chloro-indolyl phosphate (BCIP) and imaged by phase contrast light microscopy.

In situ PCR assays

Tissue sections (14 μm) were prepared from paraffin-embedded tomato stem, leaf (young and mature), and shoot apex tissues. Sections were placed onto glass slides, rehydrated, and then covered with a 25 μl aliquot of the following PCR mixture: 0.2 mM each of dATP, dCTP, dGTP, and 10 μM dTTP; 20 μM digoxigenin-labeled dTTP (Boehringer Mannheim); 2.5 mM $MgCl_2$; 3 u *Taq* polymerase (Boehringer Mannheim); and 100 μM of each primer. The primer pair used in the PCR reaction (primer sequences available upon request) directed the amplification of an ~500-bp fragment of the TYLCV C1 ORF. Sections were sealed with amplicover discs and clips (PE Applied Biosystems) and subjected to PCR (10 cycles of 94°C for 30 s, 52°C for 30 s, and 72°C for 1 min) in a Perkin–Elmer GenAmp *In Situ* Thermal PCR System-1000 (PE Applied Biosystems). Following the PCR, sections were incubated (1 min) in absolute ethanol, rinsed in 1 mM EDTA, and blocked overnight with 1% skim milk at 4°C. Sections were washed twice in phosphate buffer with Tween (PBST; 0.13 mM NaCl, 1.8 mM KH_2PO_4, 10 mM Na_2HPO_4, 2.7 mM KCl, pH 7.2, and 0.05% Tween) for 10 min. DIG-labeled DNA was detected using anti-DIG antibody (Boehringer Mannheim) conjugated to AP. The AP activity was measured using NBT and BCIP, and the chromogen produced was imaged by phase contrast light microscopy.

ACKNOWLEDGMENTS

We thank agronomy engineers Miguel Sanchez and José Jáquez (Transagricola S. A., Santiago, Dominican Republic) and Robert T. McMillen, Jr. (University of Florida) for supplying TYLCV-infected tomato tissues and Dr. Jung-Youn Lee for assistance in analysis of amino acid sequences. This research was supported in part by grants from the BARD (IS-2566–95R) and the NSF IBN-99-00539 (to W.J.L.).

REFERENCES

Azzam, O., Fraser, J., De La Rosa, D., Beaver, J. S., Ahlquist, P., and Maxwell, D. P. (1994). Whitefly transmission and efficient ssDNA accumulation of bean golden mosaic geminivirus require functional coat protein. *Virology* **204,** 289–296.

Brough, C. L., Hayes, R. J., Morgan, A. J., Coutts, R. H. A., and Buck, K. W. (1988). Effects of mutagenesis *in vitro* on the ability of cloned tomato

golden mosaic virus DNA to infect *Nicotiana benthamiana* plants. *J. Gen. Virol.* **69,** 503–514.

Carrington, J. C., Kasschau, K. D., Mahajan, S. K., and Schaad, M. C. (1996). Cell-to-cell and long-distance transport of viruses in plants. *Plant Cell* **8,** 1669–1681.

Channarayappa, Muniyapa, V., Schewegler-Berry, D., and Shivashankar, G. (1992). Ultrastructural changes in tomato infected with tomato leaf curl virus, a whitefly-transmitted geminivirus. *Can. J. Bot.* **70,** 1747–1753.

Cherif, C., and Russo, M. (1983). Cytological evidence of the association of a geminivirus with the tomato yellow leaf curl disease in Tunisia. *Phytopath. Z.* **108,** 221–225.

Cohen, S., and Antignus, Y. (1994). Tomato yellow leaf curl virus (TYLCV), a whitefly-borne geminivirus of tomatoes. *Adv. Virus Res.* **10,** 259–288.

Duan, Y. P., Powell, C. A., Purcifull, D. E., Broglio, P., and Hiebert, E. (1997). Phenotypic variation in transgenic tobacco expressing mutated geminivirus movement/pathogenicity (BC1) proteins. *Mol. Plant Microbe Interact.* **10,** 1065–1074.

Etessami, P., Callis, R., Ellwood, S., and Stanley, J. (1988). Delimitation of essential genes of cassava latent virus DNA 2. *Nucleic Acids Res.* **16,** 4811–4829.

Gardiner, W., Sunter, G., Brand, L., Elmer, J. S., Rogers, S. G., and Bisaro, D. M. (1988). Genetic analysis of tomato golden mosaic virus: The coat protein is not required for systemic spread or symptom development. *EMBO J.* **7,** 899–904.

Ghoshroy, S., Lartey, R., Sheng, J., and Citovsky, V. (1997). Transport of proteins and nucleic acids through plasmodesmata. *Annu. Rev. Plant Physiol. Plant Mol. Biol.* **48,** 27–50.

Gilbertson, R. L., Faria, J. C., Hanson, S. F., Morales, F., Ahlquist, P., Maxwell, D. P., and Russell, D. R. (1991). Cloning of the complete DNA genomes of four bean-infecting geminiviruses and determining their infectivity by electric discharge particle acceleration. *Phytopathology* **81,** 980–985.

Gilbertson, R. L., and Lucas, W. J. (1996). How do viruses traffic on the "vascular highway"? *Trends Plant Sci.* **1,** 260–267.

Grabski, S., de Feijter, A. W., and Schindler, M. (1993). Endoplasmic reticulum forms a dynamic continuum for lipid diffusion between contiguous soybean root cells. *Plant Cell* **5,** 25–38.

Heinlein, M., Padgett, H. S., Gens, J. S., Pickard, B. G., Casper, S. J., Epel, B. L., and Beachy, R. N. (1998). Changing patterns of localization of the tobacco mosaic virus movement protein and replicase to the endoplasmic reticulum and microtubules during infection. *Plant Cell* **10,** 1107–1120.

Hou, Y.-M., Paplomatas, E. J., and Gilbertson, R. L. (1998). Host adaptation and replication properties of two bipartite geminiviruses and their pseudorecombinants. *Mol. Plant Microbe Interact.* **11,** 208–217.

Hou, Y.-M., Sanders, R., Ursin, V. M., and Gilbertson, R. L. (2000). Transgenic tomato plants expressing geminivirus movement proteins: Abnormal phenotypes and delayed infection by *Tomato mottle virus* in transgenic tomatoes expressing the *Bean dwarf mosaic virus* BV1 and BC1 proteins. *Mol. Plant Microbe Interact.* **13,** 297–308.

Ingham, D. J., Pascal, E., and Lazarowitz, S. G. (1995). Both geminivirus movement proteins define viral host range, but only BL1 determines viral pathogenicity. *Virology* **207,** 191–204.

Jackson, D., Veit, B., and Hake, S. (1994). Expression of maize KNOTTED 1 related homeobox genes in the shoot apical meristem predicts patterns of morphogenesis in the vegetative shoot. *Development* **120,** 405–413.

Jeffrey, J. L., Pooma, W., and Petty, I. T. D. (1996). Genetic requirements for local and systemic movement of tomato golden mosaic virus in infected plants. *Virology* **223,** 208–218.

Johnson, D. R., Bhatnagar, R. S., Knoll, L. J., and Gordon, J. I. (1994). Genetic and biochemical studies of protein N-myristolylation. *Annu. Rev. Biochem.* **63,** 869–914.

Jupin, I., Kouchovsky, F., Jouanneau, F., and Gronenborn, B. (1994). Movement of tomato yellow leaf curl geminivirus (TYLCV): Involvement of the protein encoded by ORF C4. *Virology* **204,** 82–90.

Kasteel, D. T., Perbal, M. C., Boyer, J. C., Wellink, J., Goldbach, R. W., Maule, A. J., and van Lent, J. W. (1996). The movement proteins of cowpea mosaic virus and cauliflower mosaic virus induce tubular structures in plant and insect cells. *J. Gen. Virol.* **77,** 2857–2864.

Kikuno, R., Toh, H., Hayashida, H., and Miyata, T. (1984). Sequence similarity between putative gene products of geminiviral DNAs. *Nature* **308,** 562.

Kim, K. S., Shock, T. L., and Goodman, R. M. (1978). Infection of *Phaseolus vulgaris* by bean golden mosaic virus: Ultrastructural aspects. *Virology* **89,** 22–33.

Kotlitzky, G., Boulton, M. I., Pitaksutheepong, C., Davies, J. W., and Epel, B. (2000). Intracellular and intercellular movement of maize streak geminivirus V1 and V2 proteins transiently expressed as green fluorescent protein fusions. *Virology* **274,** 32–38.

Krake, L. R., Rezaian, M. A., and Dry, I. B. (1998). Expression of the Tomato leaf curl geminivirus *C4* gene produces viruslike symptoms in transgenic plants. *Mol. Plant Microbe Interact.* **11,** 413–417.

Kunik, T., Palanichelvam, K., Czosnek, H., Citovsky, V., and Gafni, Y. (1998). Nuclear import of the capsid protein of tomato yellow leaf curl virus (TYLCV) in plant and insect cells. *Plant J.* **13,** 393–399.

Latham, J. R., Saunders, K., Pinner, M., and Stanley, J. (1997). Induction of plant cell division by beet curly top virus gene *C4*. *Plant J.* **11,** 1273–1283.

Lazarowitz, S. G., and Beachy, R. N. (1999). Viral movement proteins as probes for intracellular trafficking in plants. *Plant Cell* **11,** 535–548.

Liu, H., Boulton, M. I., Thomas, C. L., Prior, D. A., Oparka, K. J., and Davies, J. W. (1999). Maize streak virus coat protein is karyophyllic and facilitates nuclear transport of viral DNA. *Mol. Plant Microbe Interact.* **12,** 894–900.

Liu, H., Boulton, M. I., Oparka, K. J., and Davies, J. W. (2001). Interaction of the movement and coat proteins of Maize streak virus: Implications for the transport of viral DNA. *J. Gen. Virol.* **82,** 35–44.

Lucas, W. J., and Gilbertson, R. L. (1994). Plasmodesmata in relation to viral movement within leaf tissues. *Annu. Rev. Phytopathol.* **32,** 387–411.

Lucy, A. P., Boulton, M. I., Davies, J. W., and Maule, A. J. (1996). Tissue specificity of *Zea mays* infection by maize streak virus. *Mol. Plant Microbe Interact.* **9,** 22–31.

McLean, B. G., Hempel, F. D., and Zambryski, P. C. (1997). Plant intercellular communication via plasmodesmata. *Plant Cell* **9,** 1043–1054.

Michelson, I., Zeidan, M., Zamski, E., Zamir, D., and Czosnek, H. (1997). Localization of tomato yellow leaf curl virus (TYLCV) in susceptible and tolerant nearly isogenic tomato lines. *Acta Hortic.* **477,** 407–414.

Morra, M. R., and Petty, I. T. D. (2000). Tissue specificity of geminivirus infection is genetically determined. *Plant Cell* **12,** 2259–2270.

Nagar, S., Pedersen, T. J., Carrick, K. M., Hanley-Bowdoin, L., and Robertson, D. (1995). A geminivirus induces expression of a host DNA synthesis protein in terminally differentiated plant cells. *Plant Cell* **7,** 705–719.

Nakhla, M. K., Maxwell, D. P., Martinez, R. T., Carvalho, M. G., and Gilbertson, R. L. (1994). Widespread occurrence of the eastern Mediterranean strain of tomato yellow leaf curl geminivirus in tomatoes in the Dominican Republic. *Plant Dis.* **78,** 926.

Navot, N., Picherski, E., Zeidan, M., Zamir, D., and Czosnek, H. (1991). Tomato yellow leaf curl virus: A whitefly-transmitted geminivirus with a single genomic molecule. *Virology* **185,** 151–161.

Nelson, R. S., and van Bel, A. J. E. (1998). The mystery of virus trafficking into, through and out of vascular tissue. *Prog. Bot.* **59,** 476–533.

Noris, E., Vaira, A. M., Caciagli, P., Masenga, V., Gronenborn, B., and Accotto, G. P. (1998). Amino acids in the capsid protein of tomato yellow leaf curl virus that are crucial for systemic infection, particle formation, and insect transmission. *J. Virol.* **72,** 10050–10057.

Noueiry, A. O., Lucas, W. J., and Gilbertson, R. L. (1994). Two proteins of a plant DNA virus coordinate nuclear and plasmodesmatal transport. *Cell* **76,** 925–932.

Oparka, K. J., Roberts, A. G., Boevink, P., Santa Cruz, S., Roberts, I., Pradel, K. S., Imlau, A., Kotlizky, G., Sauer, N., and Epel, B. (1999). Simple, but not branched, plasmodesmata allow the nonspecific trafficking of proteins in developing tobacco leaves. *Cell* **97,** 743–754.

Oparka, K. J., and Turgeon, R. (1999). Sieve elements and companion cells-traffic control centers of the phloem. *Plant Cell* **11,** 739–750.

Padidam, M., Beachy, R. N., and Fauquet, C. M. (1995). Tomato leaf curl geminivirus from India has a bipartite genome and coat protein is not essential for infectivity. *J. Gen. Virol.* **76,** 25–35.

Pascal, E., Goodlove, P. E., Wu, L. C., and Lazarowitz, S. G. (1993). Transgenic tobacco plants expressing the geminivirus BL1 protein exhibit symptoms of viral disease. *Plant Cell* **5,** 795–807.

Rhee, Y., Gurel, F., Gafni, Y., Dingwall, C., and Citovsky, V. (2000). A genetic system for detection of protein nuclear import and export. *Nature Biotechnol.* **18,** 433–437.

Ridgen, J. E., Dry, I. B., Mullineaux, P. M., and Rezaian, M. A. (1993). Mutagenesis of the virion-sense open reading frames of tomato leaf curl geminivirus. *Virology* **193,** 1001–1005.

Rigden, J. E., Krake, L. R., Rezaian, M. A., and Dry, I. B. (1994). ORF C4 of tomato leaf curl virus is a determinant of symptom severity. *Virology* **204,** 847–850.

Rojas, M. R. (1999). Characterization of potyvirus and geminivirus movement proteins. Ph.D. thesis, University of California-Davis.

Rojas, M. R., Gilbertson, R. L., Russell, D. R., and Maxwell, D. P. (1993). Use of degenerate primers in the polymerase chain reaction to detect whitefly-transmitted geminiviruses. *Plant Dis.* **77,** 340–347.

Rojas, M. R., Zerbini, F. M., Allison, R. F., Gilbertson, R. L., and Lucas, W. J. (1997). Capsid protein and helper component-proteinase function as potyvirus cell-to-cell movement proteins. *Virology* **237,** 283–295.

Rojas, M. R., Noueiry, A. O., Lucas, W. J., and Gilbertson, R. L. (1998). Bean dwarf mosaic geminivirus movement proteins recognize DNA in a form- and size-specific manner. *Cell* **95,** 105–113.

Russo, M., Cohen, S., and Martelli, G. P. (1980). Virus like particles in tomato plants affected by the yellow leaf curl virus disease. *J. Gen. Virol.* **49,** 209–213.

Sanderfoot, A. A., and Lazarowitz, S. G. (1995). Cooperation in viral movement: The geminivirus BL1 movement protein interacts with BR1 and redirects it from the nucleus to the cell periphery. *Plant Cell* **7,** 1185–1194.

Salati, R. (2001). Epidemiology of tomato yellow leaf curl virus in the Dominican Republic and genetic analysis of genes involved in virus movement. Ph.D. thesis, University of California-Davis.

Smith, L. G., Greene, B., Veit, B., and Hake, S. (1992). A dominant mutation in the maize homeobox gene, Knotted-1, causes its ectopic expression in leaf cells with altered fates. *Development* **116,** 21–30.

Sudarshana, M. R., Wang, H. L., Lucas, W. J., and Gilbertson, R. L. (1998). Dynamics of bean dwarf mosaic geminivirus cell-to-cell and long-distance movement in *Phaseolus vulgaris* revealed, using the green fluorescent protein. *Mol. Plant Microbe Interact.* **11,** 277–291.

Towler, D. A., Gordon, J. I., Adams, S. P., and Glaser, L. (1988). The biology and enzymology of eukaryotic protein acylation. *Annu. Rev. Biochem.* **57,** 69–99.

Von Arnim, A., Frischmuth, T., and Stanley, J. (1993). Detection and possible functions of African cassava mosaic virus DNA B gene products. *Virology* **192,** 264–272.

Wang, H. L., Gilbertson, R. L., and Lucas, W. J. (1996). Spatial and temporal distribution of bean dwarf mosaic geminivirus in *Phaseolus vulgaris* and *Nicotiana benthamiana*. *Phytopathology* **86,** 1204–1214.

Ward, B. M., Medville, R., Lazarowitz, S. G., and Turgeon, R. (1997). The geminivirus BL1 movement protein is associated with endoplasmic reticulum-derived tubules in developing phloem cells. *J. Virol.* **71,** 3726–3733.

Wartig, L., Kheyr-Pour, A., Noris, E., Kouchkovsky, F. D., Jouanneau, F., Gronenborn, B., and Jupin, I. (1997). Genetic analysis of the monopartite tomato yellow leaf curl geminivirus: Roles of V1, V2, and C2 ORFs in viral pathogenesis. *Virology* **228,** 132–140.

Zheng, H., Wang, G., and Zhang, L. (1997). Alfalfa mosaic virus movement protein induces tubules in plant protoplasts. *Mol. Plant Microbe Interact.* **10,** 1010–1014.